Local Dynamics of Chemical Kinetics at Different Phases of Nitriding Process

İ. Bedii Özdemir and Firat Akar

The local dynamics of chemical kinetics at different phases of the nitriding process have been studied. The calculations are performed under the conditions where the temperature and composition data are provided experimentally from an in-service furnace. Results are presented in temporal variations of gas concentrations and the nitrogen coverage on the surface. It is shown that if it is available in the furnace, the adsorption of the N_2 gas can seemingly start at temperatures as low as 200 °C. However, at such low temperatures, as the diffusion into the material is very unlikely, this results in the surface poisoning. It becomes clear that, contrary to common knowledge, the nitriding heat treatment with ammonia as a nitrogen-providing medium is possible at temperatures like 400 °C. Under these conditions, however, the presence of excess amounts of product gas N_2 in the furnace atmosphere suppresses the forward kinetics in the nitriding process. It seems that the best operating point in the nitriding heat treatment is achieved with a mixture of 6% N_2. When the major nitriding species NH_3 is substituted by N_2 and the N_2 fraction increases above 30%, the rate of the forward reaction decreases drastically, so that there is no point to continue the furnace operation any further. Hence, during the initial heating phase, the N_2 gas must be purged from the furnace to keep its fraction less than 30% before the furnace reaches the temperature where the reaction starts.

1. Introduction

Gaseous nitriding has been increasingly used over the past decade primarily due to the flexibility in processing parameters, which allows processed parts achieving an optimized microstructure. However, this is only possible with a tighter control of the nitriding potential which determines the nature of the solid solution to be dominated by Fe_4N (called gamma prime compound) or Fe_3N (epsilon compound). The stratification is vitally important and, when the outermost surface is covered with gamma prime compound, a crust called white layer forms, which is very brittle and requires machining (Ref 1). Unfortunately, there are currently a significant number of furnaces in use that cannot provide continuous and precise regulation of the nitriding process (Ref 2). Hence, developing new methodologies for the control of the furnace atmosphere is one of the central issues that need to be tackled (Ref 3). In an attempt to lower the processing costs and minimize the emissions, innovative process regulation concepts beyond the traditional open-loop furnace control systems must be implemented for automatic determination of temperature and the amount of gas to be delivered into the furnace over the process time (Ref 4, 5).

Control methods based on the assessing ammonia dissociation usually consist of optical gas concentration measurements in the infrared range (Ref 6). The drawbacks of this type of process regulation include the need for frequent and expensive calibration procedures and uncertainties due to the sensor drift and interference with other gases in the mixture. Furthermore, instruments used in such measurements are not always able to endure the harsh furnace environment. In order to improve robustness of a closed-loop ammonia control based on sensing the nitriding potential, it is also necessary to assess the stability of the process where removing or adjusting the excess variability in the setpoint programming present a challenging task. A continuous, accurate, and easy-to-define pathway is thus a prerequisite for model-based intelligent control algorithm of the process, which requires a reliable estimation of the local dynamics of the nitriding chemistry (Ref 7, 8).

From the system dynamics perspective, the nitriding process will be governed by a number of different time scales as much the number of species, which determine the rapidity of the reaction progress (Ref 9). The chemical system in the composition space can however be described temporally by local temperature, concentrations of gas phase species, and coverages of absorbed species on the surface, which parameterize the progress on the different branches of the solution space of the kinetics. In principle, one can find out root or manifold of the states in which the chemical source term is high enough to promote the forward progress. In the present work, local dynamics at different thermo-chemical states sampled from the nitriding pathway typically used in production plants were explored as for increasing the effectiveness and stability of the process. The results reveal some of the intricate attributes of the commonly used nitriding process and expound conduits for optimized kinetics.

İ. BediiÖzdemir and FiratAkar, Fluids Group, Faculty of Mechanical Engineering, İstanbul Technical University, Gumussuyu, 34437 Istanbul, Turkey. Contact e-mail: bozdemir@itu.edu.tr.

2. Description of the Chemistry, Numerical Method, and Sampled States

The kinetics of nitriding chemistry used in the present study (Ref 10-12) involves 11 species, including gas phase species, NH_3, H_2, and N_2, and surface species, NH_{3ad}, NH_{2ad}, NH_{ad}, N_{2ad}, H_{2ad}, N_{ad}, H_{ad}, and SUR, the latter defining the surface material itself. Twelve reactions, including adsorption, desorption, and surface reactions, form the basis of the nitriding process. As the rate laws for the reaction mechanism is depicted elsewhere (Ref 13), here it suffices to denote that R reactions among $S_g + S_a$ species can be considered as a system of first-order ordinary differential equations,

$$\frac{dm_i}{dt} = F_i\left(m_1, \ldots, m_{s_g+s_a}; k_1, \ldots, k_R\right), \quad \text{(Eq 1)}$$

subject to boundary conditions,

$$m_i\big|_{t=t_o} = m_i^o. \quad \text{(Eq 2)}$$

The mass fractions m_i of species i are the variables which depend on the time t and the parameter of the system, k_r ($r = 1,...,R$), as well as m_i^o, denoting the initial composition at t_o.

The automated composition and temperature values throughout the pathway of a nitriding cycle typically used in industry are sampled and used as the initial conditions of the

Table 1 Sampled phases of nitriding

| Sample point	1	2	3	4	5	6	7	8	9	10	11	12
Time, h	01:02	01:41	02:01	02:03	02:33	03:03	04:03	05:03	06:03	07:03	08:03	09:03
Temperature, °C	200	400	510	520	520	520	520	520	520	520	520	190
NH_3, %vol.	0	3.20	5.00	5.00	3.50	3.90	35.30	24.20	6.10	2.20	0.30	0
Y_{NH_3}	0	0.024	0.040	0.045	0.029	0.036	0.679	0.436	0.094	0.029	0.004	0
H_2, %vol.	0	19.70	25.00	34.42	27.71	35.70	58.80	61.23	62.65	57.24	54.67	21.00
Y_{H_2}	0	0.017	0.024	0.037	0.027	0.039	0.133	0.130	0.113	0.089	0.089	0.018
N_2, %vol.	100	77.10	70.00	60.58	68.79	60.40	5.90	14.57	31.25	40.56	40.03	79.00
Y_{N_2}	1	0.958	0.935	0.916	0.943	0.924	0.186	0.432	0.792	0.881	0.906	0.981
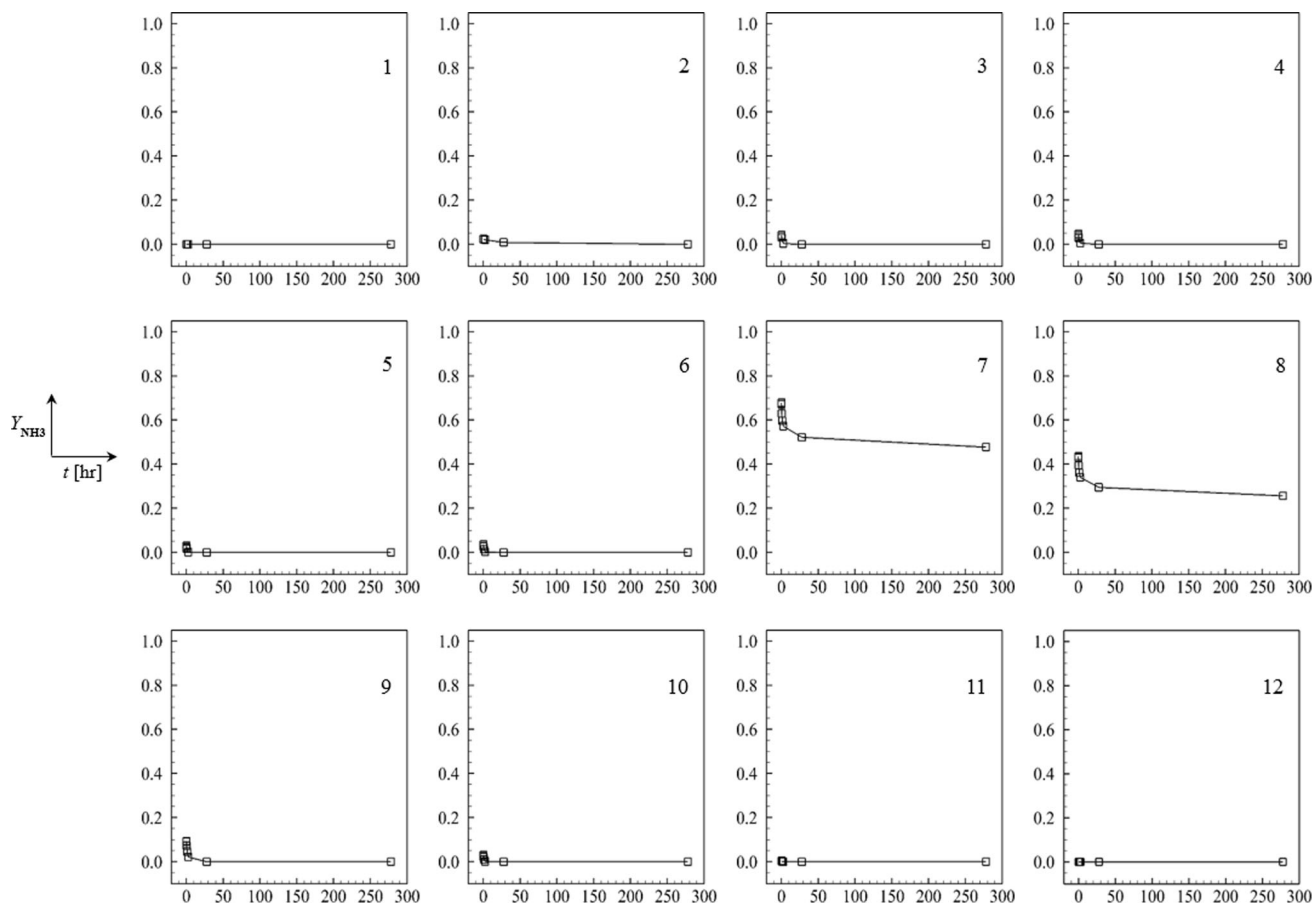
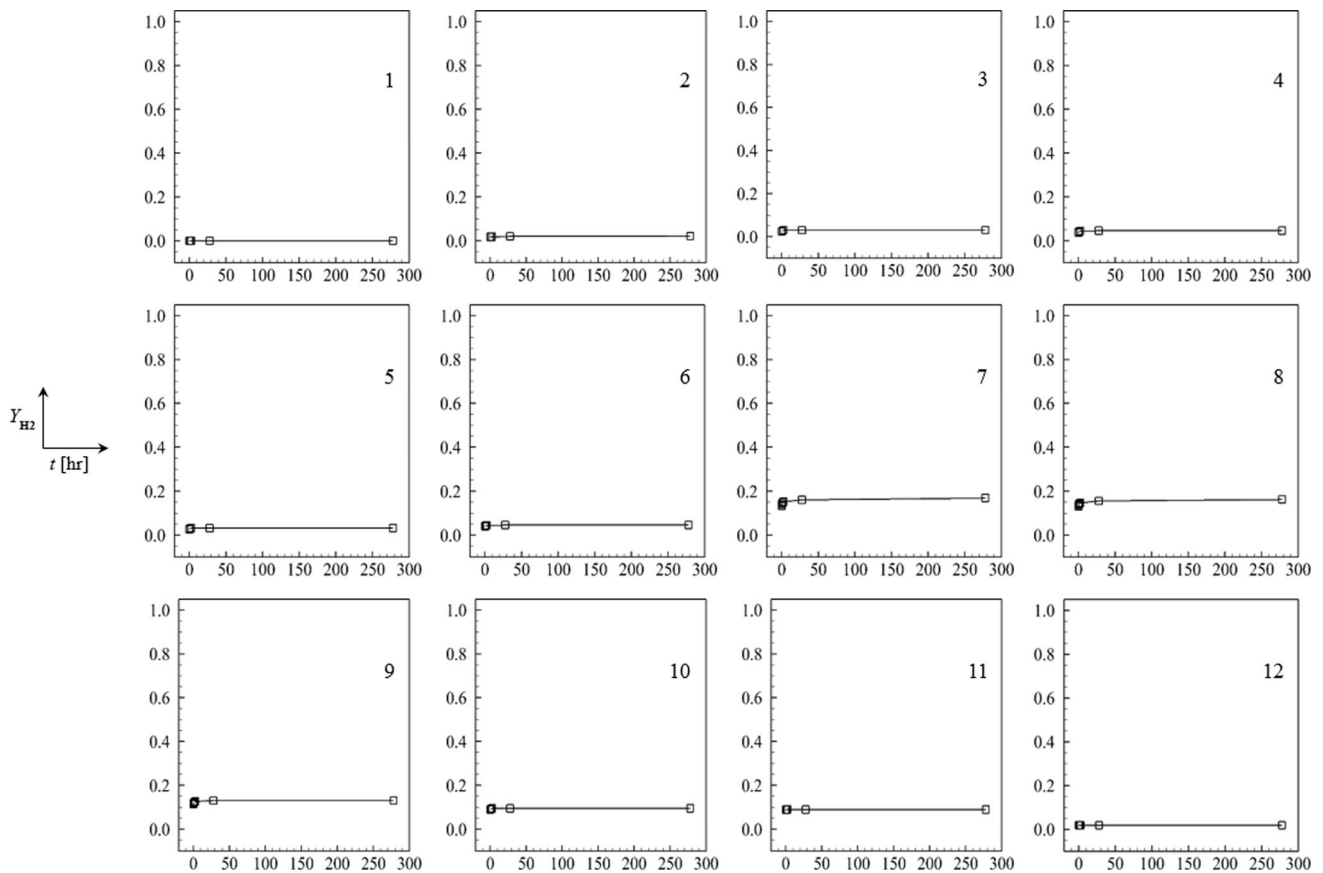**Fig. 1** Depletion of the NH_3 gas at different phases of the nitriding process

Fig. 2 Formation of the H$_2$ gas at different phases of the nitriding process

present analyses. These cycles have basically three phases: heating, main ammonia injection, and purging phases. The time-indexed temperature and composition data extracted from the pathway of an industrial furnace are shown in Table 1 where the heating phase is sampled at six different time points, each separated roughly by half an hour; the injection phase is sampled at two time points, each separated by an hour; and finally the purging phase is sampled at five time points, each separated by an hour. It is clear that the whole furnace is initially filled with N$_2$, which is then simultaneously purged and replaced with NH$_3$. The increase of H$_2$ concentration indicates that nitriding reactions are already starting even at low temperatures, which speeds up later with the main injection and then declines in the purging phase. Using the twelve sample states as the initial conditions for the subsequent time developments, the local dynamics of the pathway is studied numerically to determine the optimized kinetics manifold for the nitriding process.

The solution advance from $t_o = 0$ to t_{end} is performed by the integration of the system of differential equations (1) forward in time using an algorithm (Ref 14) which evaluates the predictor polynomial at each time step. The new solution is then computed in the corrector phase using a Newton-type iteration by solving a nonlinear system of equations. An initial step size of $\Delta t_o = 10^{-4}$ s is used to cope with the fast changes of the solution near the initial point, and thereafter, the time history of the evolution is generated with a step size of $\Delta t = 1$ s over a period of $t_{end} = 270$ h.

3. Results

Starting from the states with the conditions defined in the previous section, the progress of the reactions is calculated and the results are presented in mass fractions of species in Fig. 1, 2, 3, and 4. In each graph, the data, mass fraction versus time, are plotted linearly on the vertical and the horizontal axes, respectively. Figure 1 presents the variation of NH$_3$ concentration with time for the 12 initial states as described previously. The ammonia concentrations are either very low or entirely disappear after 100 s for the first six initial states. On curve 7, where the ammonia fraction in the local mixture is about $Y_{NH_3} = 0.68$, the progress of the nitriding process is changed distinctively: The rich ammonia content apparently enhances the reaction rate which consumes the initial amount quickly and reduces to a value of 0.48. This behavior persists for the 8th state where the ammonia concentration decays from 0.44 to 0.28. For the following two states, the decline from the initial levels of 0.08 and 0.06 becomes slower and ammonia finally disappears completely in the last three curves. It can be concluded that when the NH$_3$ concentration is high in the local mixture, the rate of its consumption seems augmented, implying the possibility of a more effective nitriding.

H$_{ad}$ is known to be the most unstable surface species and hardly diffuses into material (Ref 15). It is mostly released into the furnace atmosphere as the reaction product, H$_2$ gas, whose concentration variations with time are presented in Fig. 2.
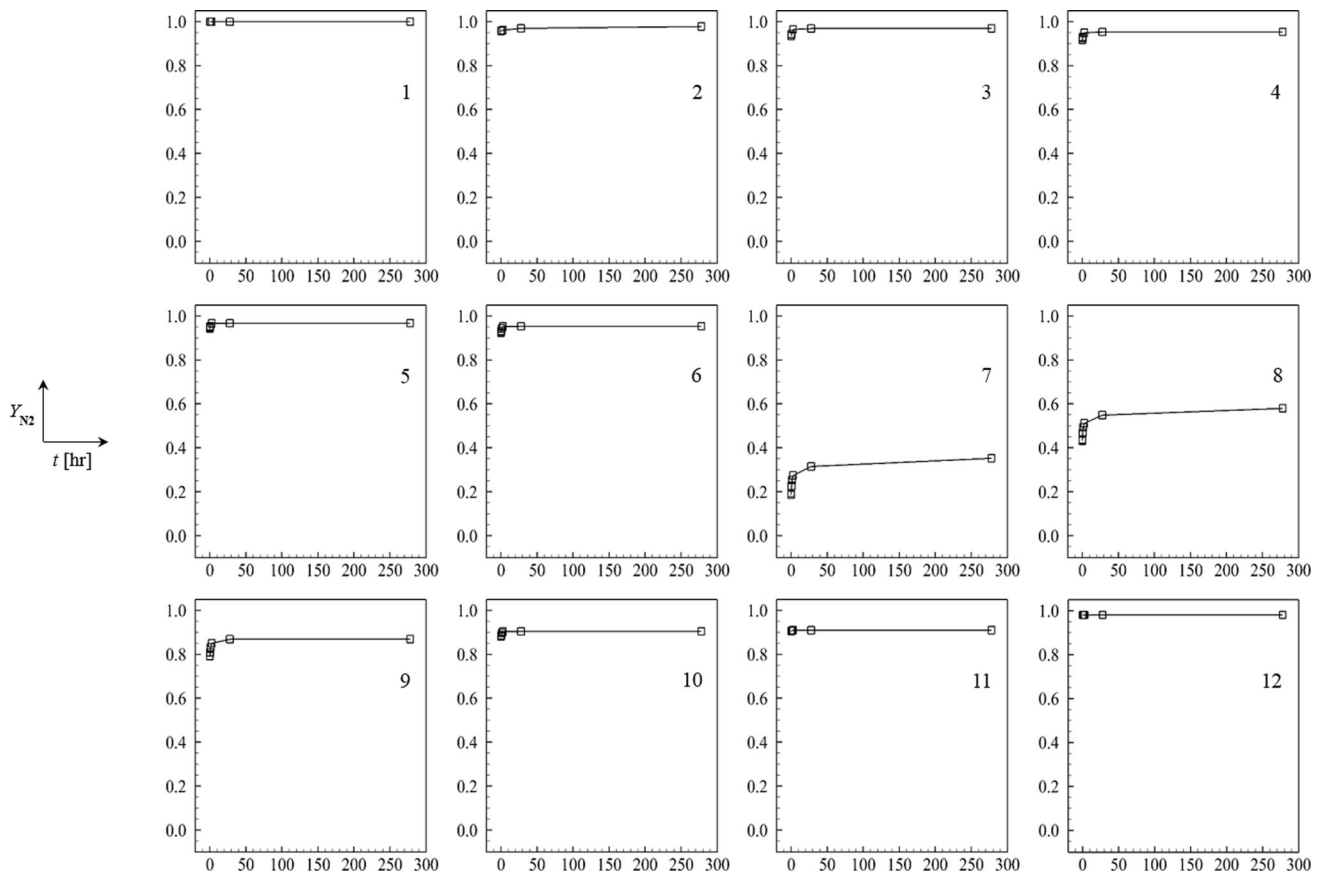
Fig. 3 Built up of N_2 gas at different phases of the nitriding process

Except for the curves 7, 8, and 9, the H_2 concentration appears very low and stays either constant or exhibits very slim rise. This is attributed to extremely slow reactions occurring at these stages due to the very low levels of ammonia (NH_3) in the furnace. However, even though the initial ammonia concentration is nearly the same, the levels of the H_2 concentrations in the curves 5 and 6 are noticeably different: The production of H_2 in the curve 6 always stays higher than the curve 5 despite the fact that the initial H_2 concentration is higher in the state 6. This shows that the presence of H_2 (as a product gas) in the initial mixture does not suppress or affect the rate of the forward reaction. The reaction speed seems to be determined basically by the N_2 concentration which is lower in the initial state of the curve 6 than the curve 5.

The curves in Fig. 3 present the changes of the N_2 mass fraction in the furnace. The first curve remains flat at the initial value because at this stage the furnace heating is just started so that no reaction occurs. The second curve starts from the condition where the ammonia (NH_3) injection has already started and the furnace temperature has reached to 400 °C so that with the initiation of the reactions, the N_2 gas starts to appear in the furnace atmosphere. This results in a reaction progress for the next four curves 3, 4, 5, and 6, where the N_2 mass fraction exhibits a steady increase. It is evident that the nitriding reactions are clearly enhanced with the conditions at the state 7 compared to those displayed in the previous curves. The state 8 begins with an N_2 concentration 0.44 and, after a relatively lower rate of increase, reaches to a value of 0.56. The starting level increases to 0.8 in the ninth state, and it rises only

to 0.85 thereafter. There appears only a slight increase of the N_2 concentration in the tenth state and, in the rest, it stays nearly constant.

Figure 4 shows the curves for the variation of the surface coverage of N_{ad} with time. The first curve on the graph indicates that there is an enormous amount of N_{ad} formation on the surface. This is surprising, since the temperature is fairly low and there is no ammonia in the furnace atmosphere yet. The apparent adsorption can only be explained by the presence of the N_2 gas: At this low temperature, once they stick to the surface, due to the insignificant mobility and energy of the atoms to break up from the surface, the coverage as high as 1 is quickly reached. But just simply because of this low temperature, it is very unlikely that the nascent nitrogen will diffuse into the material: Indeed, it is more likely that the adsorbed nitrogen will simply poison the surface. When the temperature is raised to 400 °C, and so the molecules on the surface have higher mobility and energy, the corresponding curve (curve 2) still exhibits a rapid rise, but this time it can attain a lower maximum N_{ad} coverage of 0.84 which does not remain stable and after 27 h starts decaying. The next four curves (3, 4, 5, and 6) represent the states where the temperature is continuously increased (up to 520 °C) without any increase in the supply of ammonia to the furnace. The outcome is to increase the molecular activity on the surface and hence the release of nascent nitrogens, which increases the N_2 gas in the furnace atmosphere. When the desorption process becomes equally dominant with respect to the adsorption and surface processes, the formation of N_{ad} is largely suppressed. The curve 7 is based
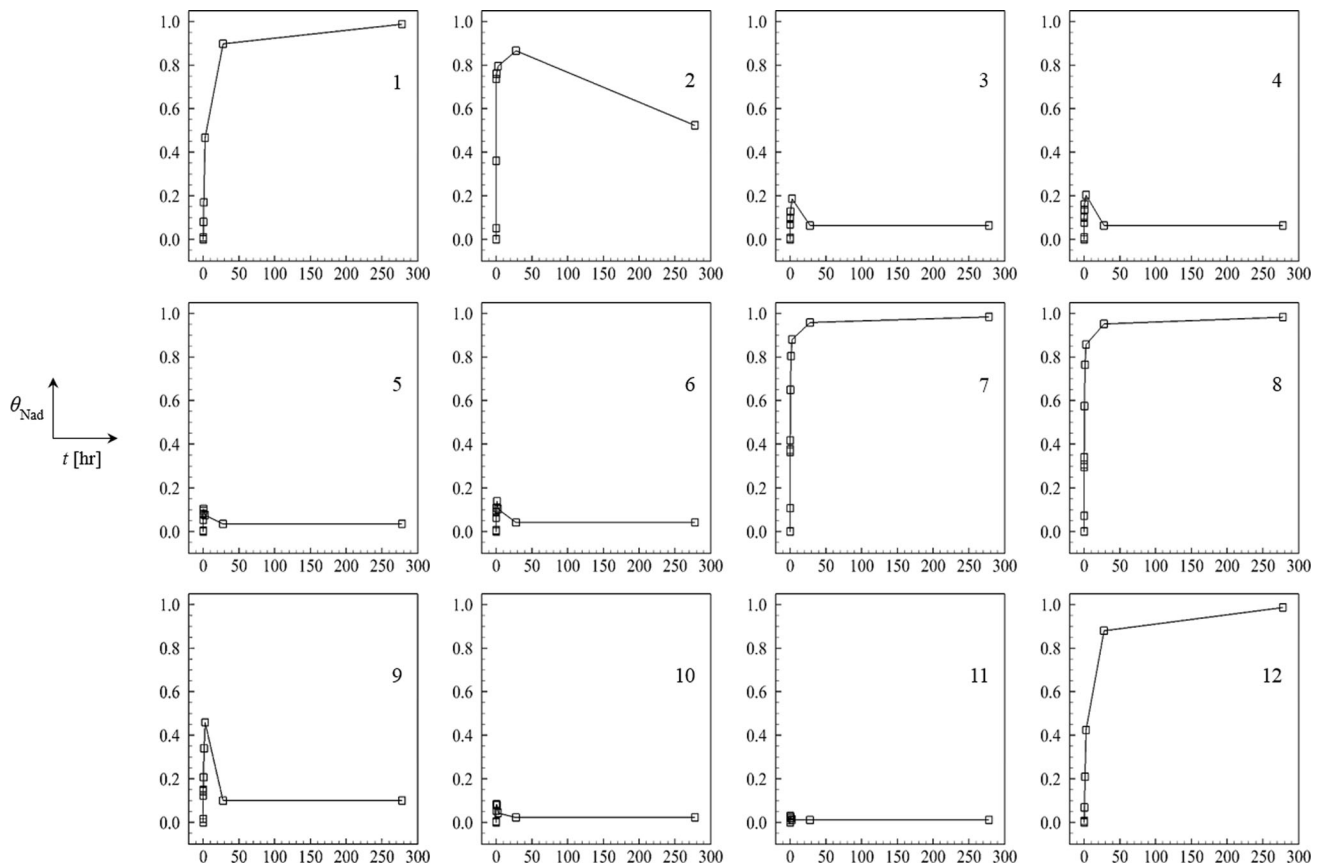
Fig. 4 Formation of N_{ad} coverage at different phases of the nitriding process

on the calculations under the process conditions with a temperature of 520 °C and NH_3 concentration of 35%. As expected, a very sharp rise occurs where the coverage on the surface reaches 0.8 within an hour and eventually attains a maximum of 1. The curve 8 duplicates nearly the same pattern but at some slower rate. In the state 9, while the initial concentration of H_2 is preserved as in the previous (state 8), the concentration of NH_3 is reduced from 24.2 to 6.1% and the concentration of N_2 is increased from 14.57 to 31.25%. These process control adjustments change the outcome drastically as shown in the curve 9: the N_{ad} coverage increases rather slowly and, after an hour, it develops only half of the value of the state 8 (0.44), which then sharply decreases to 0.1. It can be inferred that the main reason for such different trends is the increase in the concentration of N_2 gas in the furnace atmosphere, which inhibits the surface reactions that eventually produces atomic nitrogen, part of which is likely to diffuse into the material and the rest is released through the desorption into the furnace. The N_{ad} formation in the remaining states 10 and 11 gradually ceases. The increase in the N_{ad} formation in the last curve is associated with the low temperature absorption process of N_2 gas on the surface, since NH_3 is no longer available.

4. Conclusion

In multi-component furnace atmospheres, the composition of gases seems to be critically important for the effectiveness of

the nitriding process: the local dynamics reveal that presence of product gas N_2 in the furnace atmosphere severely inhibits the forward kinetics. The mixture with 6% N_2 content proves to be the best composition for the fast and efficient nitriding operation, and when N_2 fraction is increased from this point, the favorable situation deteriorates and, finally above 30%, the nitriding potential nominally diminishes. The results of kinetics study also show that the surface reactions are working at temperatures as low as 200 °C. However, when the furnace atmosphere is made up of N_2 only, for the temperatures below 400 °C, the adsorption occurs predominantly by the sticking of the N_2 gas, which poisons the surface and adversely affects the nitriding potential. Therefore, it is concluded that if the furnace is filled with N_2 at the beginning of operation, it must be purged by a continuous supply of NH_3 to a level less than 30% before the furnace temperature reaches 400 °C.

References

1. E.J. Mittemeijer, Fundamentals of Nitriding and Nitrocarburizing, Steel Heat Treating Fundamentals and Process, *ASM Handbook*, J. Dossett and G.E. Totten, Ed., ASM International, Ohio, 2013, p 619–646
2. K.M. Winter, Gaseous Nitriding: In Theory and In Real Life. *Proceedings of the 25th Conference of the ASM Heat Treating Society*, Indiana, September 14–17, 2009
3. L. Maldzinski, W. Liliental, G. Tymowski, and J. Tacikowski, New Possibilities For Controlling Gas Nitriding Process by Simulation of Growth Kinetics of Nitride Layers, *Surf. Eng.*, 1999, **15**, p 377–384

4. L. Maldzinski, Controlled Nitriding Using a Zeroflow Process, *Heat Treat. Prog.*, 2007, **7**(5), p 53

5. K.M. Winter, S. Hoja and H. Klümper-Westkamp, State-of-the-Art Controlled Nitriding and Nitrocarburizing, United Process Control, Tech004, 2010, p 1–11

6. J. Ratajski, R. Olik, T. Suszko, J. Dobrodziej, and J. Michalski, Design, Control and In Situ Visualization of Gas Nitriding Process, *Sensors*, 2010, **10**, p 218–240

7. H.J. Grabke, Conclusions on the Mechanism of Ammonia-Synthesis from the Kinetics of Nitrogenation and Denitrogenation of Iron, *Z. Phys. Chem. Neue Folge*, 1976, **100**, p 185–200

8. R.E. Schacherl, P.C.J. Graat, and E.J. Mittemeijer, Nitriding Kinetics of Iron-Chromium Alloys; The Role of Excess Nitrogen; Experiments and Modelling, *Metall. Mater. Trans. A*, 2004, **35**, p 3387–3398

9. S.K. Upadhyay, *Chemical Kinetics and Reaction Dynamics*, Springer, New York, 2006

10. I.B. Özdemir and N. Lippmann, Modeling and Simulation of Surface Reactions and Reactive Flow of a Nitriding Process, *Surf. Coat. Technol.*, 2013, **219**, p 151–162

11. I.B. Özdemir and F. Akar, The Effect of Flow Orientation on Nitriding Process, *Vacuum*, 2015, **116**, p 104–109

12. I.B. Özdemir and F. Akar, The Response of Nitriding Chemistry to Different Initial Gas Compositions, *J. Mater. Eng. Perform.*, 2015. doi:10.1007/s11665-015-1585-z

13. R.J. Kee, M.E. Coltrin, and P. Glarborg, *Chemically Reacting Flow: Theory and Practice*, Wiley, Hoboken, 2005

14. R.S. Maier, L.R. Petzold, and W. Rath, Parallel Solution of Large Differential-Algebraic Systems, *Concurrency*, 1995, **7**, p 795–822

15. A.D. Boese, A. Chandra, J.M.L. Martin, and D. Marx, From Ab Initio Quantum Chemistry to Molecular Dynamics: The Delicate Case of Hydrogen Bonding in Ammonia, *J. Chem. Phys.*, 2003, **119**, p 5965–5980